doi:10.1111/evo.14350

Rapid microgeographic evolution in response to climate change

A. Z. Andis Arietta[1,2] **and David K. Skelly**[1]

[1] *School of the Environment, Yale University, New Haven, Connecticut 06520*

[2] *E-mail: a.andis@yale.edu*

Received April 28, 2021

Accepted August 27, 2021

Environmental change is predicted to accelerate into the future and will exert strong selection pressure on biota. Although many species may be fated to extinction, others may survive through their capacity to evolve rapidly at highly localized (i.e., microgeographic) scales. Yet, even as new examples have been discovered, the limits to such evolutionary responses have not often been evaluated. One of the first examples of microgeographic variation involved pond populations of wood frogs (*Rana sylvatica*). Although separated by just tens to hundreds of meters, these populations exhibited countergradient variation in intrinsic embryonic development rates when reared in a common garden. We repeated this experiment 17 years (approximately six to nine generations) later and found that microgeographic variation persists in contemporary populations. Furthermore, we found that contemporary embryos have evolved to develop 14–19% faster than those in 2001. Structural equation models indicate that the predominant cause for this response is likely due to changes in climate over the intervening 17 years. Despite potential for rapid and fine-scale evolution, demographic declines in populations experiencing the greatest changes in climate and habitat imply a limit to the species' ability to mitigate extreme environmental change.

KEY WORDS: amphibian, countergradient variation, evolutionary rescue, extinction, global warming, local adaptation.

The pace of environmental change experienced by contemporary wildlife populations is unprecedented and expected to accelerate (Sala et al. 2000; Urban 2015). Although climate and habitat change will exert strong selection pressure, we lack an understanding of the rate at which plastic and genetic adaptation can keep pace with environmental change (Gienapp et al. 2008; Hoffmann and Sgrò 2011; Meester et al. 2018). Currently, most models of extinction risk fail to account for adaptation and fine-grained variation, which could drastically alter predicted risks (Urban 2015) and inform management decisions (Gaitán-Espitia and Hobday 2020).

Countergradient variation, wherein organisms' phenotypes counter environmentally induced effects along a gradient such as temperature, indicates a remarkable ability for traits to be fine-tuned to local conditions even when phenotypes vary relatively little in situ (Conover and Schultz 1995). Common garden experiments that compare populations from across environmental gradients in a common setting have shown that genetic (as opposed to plastic) variation can account for a substantial portion of a population's ability to buffer environmental effects (e.g., Berven et al. 1979; Orizaola et al. 2010; Muir et al. 2014), even at surprisingly small scales (Skelly 2004; Ficetola and Bernardi 2005; Richardson et al. 2014). In addition to uncovering evolutionary divergence at small spatial scales, recent research indicates that ecologically relevant evolution can occur over short time scales, as well (Hendry and Kinnison 1999; Reznick et al. 2019). Although the intersection of fine-grained and rapid adaptation remains largely unexplored, this phenomenon prompts hope in the capacity of natural populations to react to contemporary, often anthropogenic, environmental change (Hoffmann and Sgrò 2011; Razgour et al. 2019). However, it is unclear if organisms can keep pace with such manifold changes (Carlson et al. 2014; Catullo et al. 2019).

Declining populations may avoid extinction through rapid adaptation—a process termed evolutionary rescue (Gomulkiewicz and Holt 1995). However, there are limits to a population's ability to adapt (Meester et al. 2018; Klausmeier et al. 2020). Contemporary climates are changing at an unprecedented

pace, whereas at the same time, land-use change alters habitat composition. For evolutionary rescue to occur, adaptive alleles must increase in a population fast enough to avoid falling below a demographic threshold where stochastic processes make extinction likely (Carlson et al. 2014). Populations that are slow to adapt remain below this threshold longer and are more likely fated to extinction (Gomulkiewicz and Holt 1995). In heterogeneous landscapes, influxes of migrants from nearby dissimilar habitats can introduce maladapted alleles and protract the time a population remains below the demographic threshold, as well (Bolnick and Nosil 2007; Schiffers et al. 2013). Thus, the coincidence of rapid adaptation at microgeographic scales is expected to facilitate evolutionary rescue.

One of the first examples of microgeographic countergradient variation was demonstrated in development rates of wood frogs (*Rana sylvatica*) with respect to a gradient of canopy openness (Skelly 2004). As in most ectotherms, development rates of aquatic wood frog larvae are strongly influenced by water temperatures of their resident ponds. Canopy structure has large impacts on the ecology of temporary wetlands (i.e., vernal pools) in which wood frogs breed (Werner et al. 2007). Canopy closure partially mediates pond water temperature through shading, and can alter hydroperiod via evapotranspiration, limiting the duration of the developmental window of aquatic larvae (Brooks and Hayashi 2002).

In Skelly's (2004) common garden experiment, wood frogs from dark, ostensibly colder, ponds exhibited faster embryonic development than conspecifics from warm, open ponds separated by tens to hundreds of meters. The interpretation of these results was that faster intrinsic development confers a fitness advantage in shaded ponds, allowing larvae to advance into the terrestrial life-stage prior to ponds drying up and in relative synchrony with competing warm-pond conspecifics after metamorphosis.

Although common garden experiments and other synchronic comparisons (i.e., comparing populations across space at the same time) are powerful tools to infer evolutionary divergence, they cannot provide direct evidence of evolutionary response to climate change, which is inherently a change over time (Kawecki and Ebert 2004; Merilä and Hendry 2014). Repeating common-garden studies across time allows for allochronic comparisons (i.e., comparing the same populations at different times) to directly associate changes in the environment with the genetic component of phenotypic change (e.g., Bradshaw and Holzapfel 2001; Nevo et al. 2012).

In the intervening decades since Skelly's (2004) experiment, ambient annual temperatures experienced by wood frog populations at the site have increased by 0.6°C (Arietta et al. 2020), which is likely to have similarly warmed the water temperature of natal ponds. The climate has also become more variable and extreme. For example, drought conditions between 2015 and 2017 were some of the most extreme of the last century, second only to the catastrophic drought of the 1960s that caused crop failure and water shortages across the nation (Rowland et al. *in review*). The forest canopies above wood frogs' natal ponds are likely to have changed, too. Disturbances such as blowdowns and forest clearing by beaver or humans can immediately and drastically increase light penetration to vernal pools. Conversely, as the composition of shoreline vegetation changes and individual plants mature, canopies can quickly shade ponds within two decades. Thus, this system offers a unique opportunity to test for rapid, microgeographic evolution to contemporary climate and habitat changes.

In this experiment, we repeat a common garden experiment from 2001 (Skelly 2004) with as much fidelity as possible to the original experiment (e.g., following the same protocol, using the original lab equipment, testing the same populations) and reanalyze the original data to compare to our contemporary results. We first evaluate whether wood frogs maintain microgeographic variation in development rates with respect to canopy or pond temperature after 17 years. Countergradient variation offers somewhat of a paradox for predicting responses to climate change in contexts in which adaptive alleles could be easily shared among all populations in a handful of generations. For microgeographic countergradient variation to persist, there must be not only directional selection for a trait at one end of the gradient, but also selection against that trait at the opposite end. Otherwise, the pattern would erode as populations at one extreme benefited from intrinsic and extrinsic effects in the same direction. In the case of development rates, tradeoffs with performance have been invoked to explain microgeographic countergradient variation (Gahm et al. 2021). Over time, environmental change shifts the range of the gradient experienced by populations, setting more populations up against tradeoff thresholds. Unless further adaptation shifts the threshold for tradeoffs, we would expect microgeographic countergradient patterns to further erode.

Second, we test for environmental change in pond water temperature and canopy closure between experimental timepoints. Third, we test for demographic and evolutionary response of wood frogs to recent environmental change by allochronic comparison of intrinsic embryonic development between experimental cohorts. We use structural equation models to decouple the direct impacts of environmental change and parental effects on changes in developmental timing. We hypothesize that if rapid local adaptation has occurred, the magnitude of trait change in a population should correspond to the magnitude of local environmental change, which varied among ponds.

Finally, we relate population growth or decline to the degree of environmental change. If there are limits to evolutionary rescue, we hypothesize that populations experiencing greater environmental change will exhibit negative population growth.

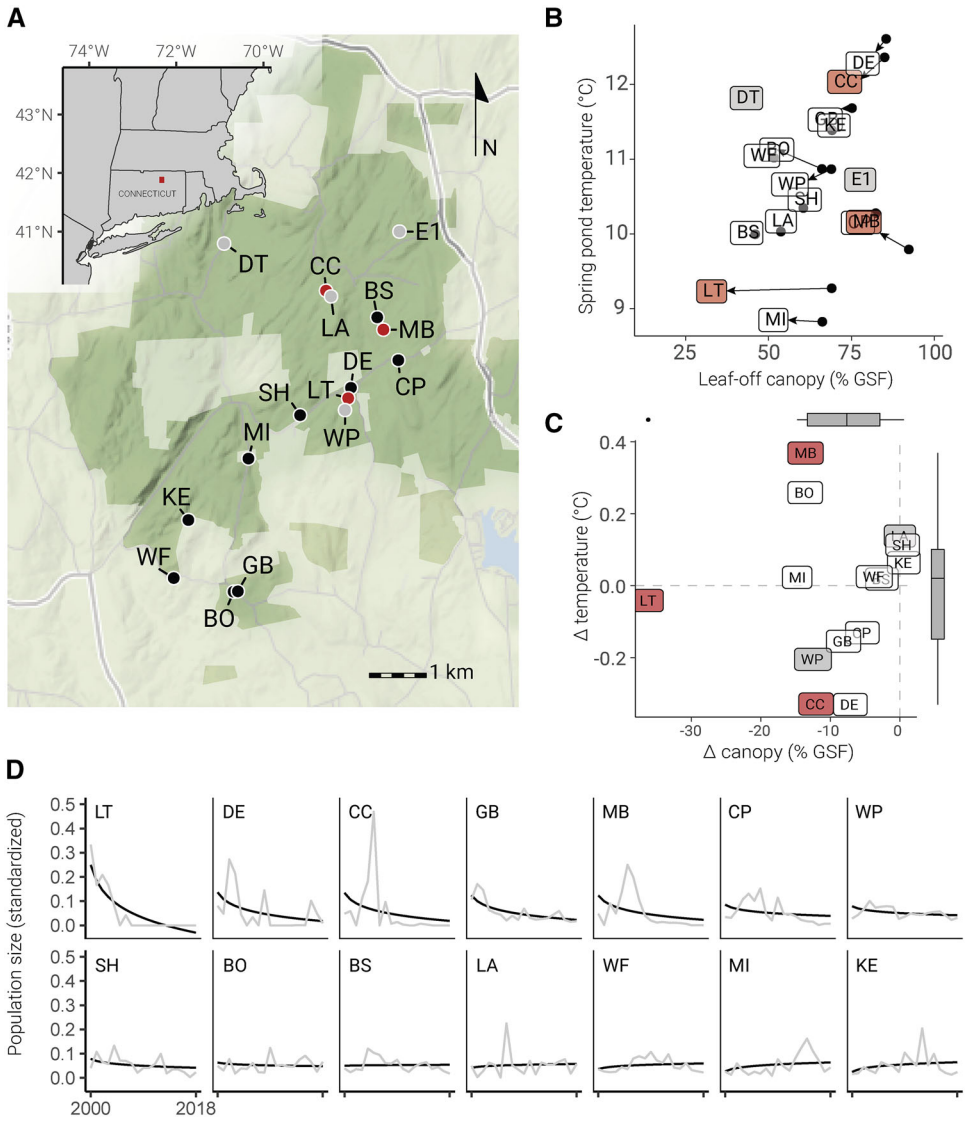

Figure 1. **Embryonic development rates and natal pond environment were measured for 16 wood frog breeding populations (A). Cohorts sampled in both 2001 and 2018 for nine ponds were included in the experiment . Three ponds that were included in the 2001 experiment ceased to host breeding populations in 2018 (red) and four additional populations were included in the 2018 experiment (gray). Absolute (B) and relative (C) change in leaf-off canopy closure (measured as percent global site factor) and water temperature during the embryonic period (day-of-year 91 to 135) are shown for those ponds with records. Marginal distribution of environmental change is indicated by the box plots in (C). Population trends (D) are reported as relative proportion of total population counts egg mass counts from 2000 to 2018 (gray lines), with logarithmic growth curves for each population (black lines).**

Methods

EMBRYO COLLECTION AND CARE

In the spring of 2018, we conducted a common garden experiment following the methods in Skelly (2004). We collected embryos from 13 wood frog breeding ponds at Yale Myers Forest, Connecticut, USA (Fig. 1A) within 24 hours of oviposition between 31 March and 14 April 2018. Nine of these ponds overlap with those studied in the 2001 experiment. Three of the ponds (MB, CC, LT) included in the previous study did not host breeding aggregations in 2018. We added four ponds (DT, E1, LA, WP) not included in 2001 to represent the range of canopy and temperature gradients present across our field site (Fig. 1B). As in 2001, we collected 12 embryos from each of up to six clutches, with the exception of "LA" pond, from which we collected embryos from two clutches due to stocking space limitations.

We excised embryos from the egg mass, being careful not to puncture the vitelline membrane, and placed them individually into wells of six-well culture plates with 15 mL reconstituted distilled water so that each plate contained six full-sib embryos. We split clutches across two temperature treatments (high:

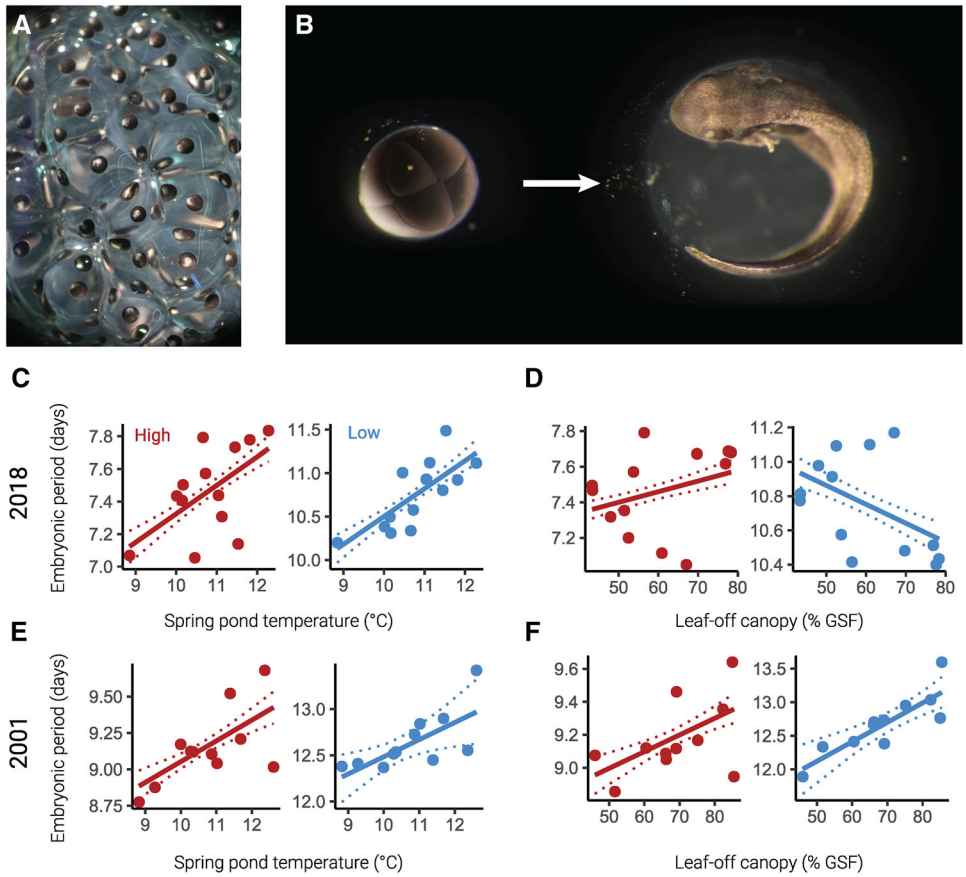

Figure 2. **Embryonic periods were estimated by rearing individual embryos excised from wood frog egg masses (A) and fitting development rate models to Gosner (1960) stages assigned from photographs taken of embryos between oviposition and hatching (B). Countergradient variation was assessed by regressing estimated embryonic periods against pond water temperature and canopy closure values for each cohort with mixed-effect multiple regression. The partial effects of pond water temperature (C, E) while holding canopy constant and canopy (D, F) while holding temperature constant are shown for embryos in the high (red) and low (blue) temperature treatments. Points indicate mean population-wise estimates (model fit + conditional residuals). Note that 95% confidence intervals (dashed lines) for the regression line were estimated by fitting the models to 1000 nonparametric bootstrap replicates.**

13.7°C; low: 11.7°C). Incubator temperatures were set to replicate the original study and represent a large portion of the range in temperatures measured at wood frog oviposition sites. We stocked one plate from each clutch into each light controlled incubator treatment with a 12:12 h photoperiod centered at 1200 EST. The incubators (I-36VL; Percival Scientific, Inc.) were the same units used in the original study. Plates were placed randomly in the incubators and rotated daily. In total, we included 888 embryos representing 74 clutches in the experiment.

We monitored embryos daily and estimated hatching as the moment when a larva breaks through the vitelline membrane. Embryos that died or exhibited abnormal development were noted and excluded from further analysis.

EMBRYONIC PERIOD AND EMBRYO VOLUME

We photographed embryos upon stocking, twice during larval development, upon hatching, and three days posthatch to record developmental stages (Fig. 2B). From these photos, we estimated developmental stage (Gosner 1960) and size. We estimated initial embryo size as the spherical volume of the mean diameter measured on the *x* and *y* axis in ImageJ (v 1.51k; Schneider et al. 2012). This protocol follows Skelly (2004) with one modification, whereas Skelly (2004) did not include photos taken after hatching; we included photos taken up to three days posthatch to make up for 123 individuals who were not photographed immediately upon hatching.

Because embryos varied in initial stage and hatching stage, we standardized embryonic period estimates by fitting a logarithmic mixed effect regression model of development rate to predict the elapsed time between Gosner stage 1 (fertilization) and 20 (hatching) while correcting for the slight difference in realized treatment temperatures between experimental years (11.3°C and 13.4°C in 2001 vs. 11.7°C and 13.7°C in 2018) (eq. 1). To do so, we estimated a parameter for incubator

temperature and held this parameter value constant at the midpoint between years (low = 11.50°C, high = 13.55°C) when predicting embryonic periods. This correction assumes that the reaction norm of temperature on development is linear over the 0.3–0.4°C interval of difference between experiments (Fig. S8).

We fit our models by regressing the embryonic stage on the interaction between the natural log of days since oviposition (*Day*) and incubator temperature (*IncTemp*) (eq. 1). We considered the collection date as day 1. We included random intercepts for each clutch (j) nested within pond (k) and random slopes for individuals (i) nested within clutch (j), respective of treatment group (l) that were uncorrelated with the intercept. This specification assumes that all embryos from the same clutch were fertilized at the same time, accounts for repeated measures of individuals, and accounts for nested data structure. Here, our analysis departs from Skelly (2004) who fit logarithmic models of development rate to each embryo, independently. To compare datasets, we re-estimated embryonic periods for the 2001 experiment using our model. Pond "MB" was excluded from the 2001 dataset as an outlier following Skelly (2004), because it was assumed that these individuals represented first-generation immigrants from nearby ponds.

$$\text{Stage} = \beta_0 + \beta_1 \ln \text{Day} + \beta_2 \text{IncTemp} + \beta_3 \ln \text{Day} \cdot \text{IncTemp} + b_{0_k} + b_{1_{jk}} + b_{2_{jkl}} \ln \text{Day} + b_{3_{ijkl}} \ln \text{Day} + \varepsilon \quad (1)$$

All regression models in this study were fit with lme4 (version 1.1.23; Bates et al. 2015) with 95% confidence intervals for model parameters estimated from 1000 nonparametric bootstrap iterations. Marginal and conditional pseudo-R^2 values were estimated with MuMIn (version 1.43.17; Barton 2019).

CANOPY

We estimated canopy closure as the ratio of above-canopy radiation to below-canopy radiation expressed as a percent. This ratio, termed global site factor (GSF) ranges from 0% to 100% (i.e., complete closure to completely open) (Anderson 1964). We estimated GSF values from hemispherical photos of the leaf-off canopy (i.e., prior to deciduous leaf emergence) with Gap Light Analyzer (Frazer et al. 1999), by plotting a sun path over the hemispherical images and integrating incident radiation from day-of-year 91–135 (approximately April 1 to May 15), as in Skelly (2004). In addition, we estimated GSF over the duration of the larval period for the duration of April 1 through August 30 as the weighted average of the leaf-on and leaf-off estimates with respect to the proportion of days before and after leaf emergence (May 15).

Skelly (2004) estimated canopy closure in 2001 from multiple photos taken at 5 m intervals along a cartesian grid. In 2018, we captured five photos for each pond—four photos 1 m in from the springtime shoreline at each cardinal point and one photo in the center. To compare canopy estimates across timepoints, we subsampled the five grid points corresponding to the cardinal point and pond center and recalculated mean GSF. These subsampled estimates tightly correlate with those including all photos from the grid ($R^2 = 0.93$) (see Supporting Information 1). We averaged these five estimates for pond-wise values and compared closure estimates for 14 ponds with data from 2001 and 2018, including all nine ponds in the embryonic development experiments. We used a paired t-test to test for a site-wide change in canopy closure over time.

WATER TEMPERATURE

Temperature is directly related to development rates in amphibians. However, at the time of the 2001 experiment, no long-term temperature data were available to parse the relative impacts of temperature or canopy gradients. Starting in 2001, we recorded water temperatures in a subset of the 60 wood frog breeding ponds at our field site. We recorded water temperature at the deepest point in the pond every 0.5 or 1 h with submersible temperature loggers (HOBO 8K Pendant; Onset Computer Corporation) suspended 10 cm below the surface. Loggers were deployed within days of oviposition and removed after larvae had metamorphosed or the pond dried. We use these data to estimate long-term water temperature gradients among our ponds.

Because we did not record water temperature in all ponds included in this study in all years, we imputed missing temperature values with a random forest model implemented in randomForest (version 4.6.14; Liaw and Wiener 2002) trained on all ponds at our site. Regression trees included both climate and site predictor variables. Climate variables included daily maximum, minimum, and average temperature, radiation, precipitation, snowpack, and atmospheric pressure from the Daymet database (version 3; Thornton et al. 2016). We included a one-day lag for all climate variables. Site variables included elevation, aspect, latitude, mean and variance of leaf-on and leaf-off GSF, and a factor for individual ponds (see Supporting Information 2).

We grew our random forest from 300 regression trees and used 10-fold cross-validation to evaluate the predictive accuracy for imputed points. Combining observed and imputed daily temperature values allowed us to calculate annual mean temperatures for the spring, leaf-off period (day-of-year 91–135) and approximate larval period (day-of-year 91–168). We combined these values for the three years preceding each experiment (i.e., 1998–2000 for 2001 and 2015–2017 for 2018) into a single average temperature value. This timespan captures the average temperatures experienced by the parental cohort and reflects long-term heterogeneity in temperature among ponds without year-to-year variation.

COUNTERGRADIENT VARIATION

We tested for countergradient variation and estimated the effects of canopy and pond water temperatures on the duration of embryonic period by fitting linear mixed models with embryonic period as the dependent variable. For each experimental cohort, we fit multiple models including combinations of canopy, pond water temperature, and the interaction. All models included an interaction term to allow the effect along the environmental gradient to vary between incubator temperature treatments and random intercepts for pond of origin. We fit the same models using environmental variables estimated for seasonal windows encompassing the embryonic and larval period but results did not differ substantially (Table S5, Fig. S9). Clutch membership was not included as a random effect in these models as the variance among siblings was accounted for in the best linear unbiased predictors of the development rate model used to estimate embryonic periods. We consider a significant and positive relationship between embryonic period and pond temperature or canopy openness as evidence of countergradient variation.

TEMPORAL COMPARISONS

We combined the embryonic period and embryo volume estimates with the environmental datasets generated in the synchronic analyses into an allochronic dataset to test for evolution in embryonic development across time. Change in canopy and temperature were estimated as the pond-wise difference between 2018 and 2001 values as described above.

We estimated population-wise evolutionary rates in *haldanes* following equations in Kinnison and Hendry (2001). We estimated change in developmental rates by subtracting the individual values of embryonic period in 2001 from pond-wise means in 2018, and the reverse (i.e., individual 2018 traits minus pond-wise 2001 means). We then estimated clutch-wise values as the mean among siblings within each temperature treatment for further analysis.

We built structural equation models (SEM) to test how the magnitude of changes in canopy, temperature, and embryo volume impact the shifts in embryonic period, given an a priori causal model (Table S6). Our causal path model was predicated on the hypothesis that changes in canopy, temperature, and/or embryonic volume may have directly induced a response in intrinsic embryonic development. We further hypothesized that the change in embryo volume may be a response to change in canopy and/or temperature. Finally, we hypothesized that change in pond temperature may be a result of changes in canopy. We fit our SEMs as a piecewise model with paths estimated as locally independent relationships in piecewiseSEM (version 2.1.0; Lefcheck 2016). We fit an identical SEM for each temperature treatment.

LIMITS OF EVOLUTIONARY RESPONSE

There may be a point at which the pace of environmental change outpaces wood frogs' ability to respond, leading to demographic effects, and ultimately, extirpation of breeding populations. In fact, three ponds ceased to host breeding populations between experimental cohorts. We tested for a correlation between environmental change and demographic decline using annual egg clutch counts. Because each female produces only a single clutch each year, these surveys serve as an excellent index of the size of the female breeding population (Berven 2009). Briefly, egg mass counts were conducted in all ponds within one week after oviposition. As wood frogs are explosive breeders, this timing ensures that all oviposition has ceased but egg masses are not too swollen to identify distinct clutches. Ponds were completely searched by two observers whose independent counts were then averaged (see detailed methods in Arietta et al. 2020).

We assessed the relationship between environmental change and population growth in a mixed model framework. We regressed logarithmic population growth curves—annual egg mass counts (scaled to population size) against the log-transformed year—allowing the slopes to vary with total environmental change via an interaction parameter. We computed a single metric of environmental change by dividing pond water temperature and canopy measures by their respective standard deviations and summing their absolute values. We modeled the variance in growth curves among pond as random effects and assessed significance of parameter estimates with 1000 nonparametric bootstraps. Thus, a significant parameter estimate for the interaction between environmental change and the log-transformed year would indicate a relationship between the magnitude of environmental change and the rate of population growth or decline.

Results

EMBRYONIC DEVELOPMENT AND SIZE

In total, we stocked 888 embryos into the 2018 experiment. Mortality was low ($n = 31$) with 96% survival in the high temperature treatment and 97% survival in the low treatment. We removed 46 (5%) observations from the dataset due to deformities or irregularities during development and six due to missing data (1%). In total, we retained 805 embryos (91%) in the analysis (high: $n = 405$, low: $n = 400$).

Of the 780 embryos included in the 2001 experiment, 59 (8%) were excluded because the embryo did not survive to hatch ($n = 58$), or due to missing data ($n = 1$). Embryos from "MB" pond ($n = 47$) were determined to be outliers by Skelly (2004), and therefore, were not included in the countergradient analysis. "MB" pond did not host a breeding population in 2018, and so, does not pertain to the allochronic analysis. In total, 674 embryos

Table 1. Results of a mixed-effect regression of embryonic development with random intercepts for clutch-mates and random slopes for individuals nested within clutch fit to data from the 2018 experiment ($N_{observation}$ = 3186, $N_{individual}$ = 805, N_{clutch} = 146, N_{pond} = 13) and 2001 experiment ($N_{observation}$ = 3971, $N_{individual}$ = 721, N_{clutch} = 128, N_{pond} = 12). Significant parameter estimates for which 95th percentile confidence intervals from 1000 non-parametric bootstraps do not contain zero are shown in bold.

	Stage (2018)			Stage (2001)		
Predictors	Estimates	CI	*P*	Estimates	CI	*P*
Intercept	**4.04**	**2.79–5.31**	**<0.001**	**3.59**	**2.71–4.56**	**<0.001**
ln(Day)	1.32	–0.35 to 2.91	0.13	**2.84**	**1.63–4.01**	**<0.001**
IncTemp	**0.15**	**0.08–0.21**	**<0.001**	**0.32**	**0.26–0.37**	**<0.001**
ln(Day) * IncTemp	**0.40**	**0.28–0.53**	**<0.001**	**0.19**	**0.10–0.29**	**<0.001**
Random effects				**Random effects**		
σ^2	1.13			0.60		
$b_{0\ Pond}$	2.27			1.32		
$b_{1\ Clutch:Pond}$	1.90			1.06		
$b_{3\ Inc:Pond:Clutch*lnDay}$	0.58			0.35		
$b_{4\ Inc:Pond:Clutch:ID*lnDay}$	0.00			0.00		
Marginal R^2/conditional R^2	0.87/0.98			0.825/0.976		

Fixed effect predictor variables include the natural log transformed days since stocking (ln(Day)), the realized incubator temperature in °C (IncTemp), and the interaction. These models were used to predict the duration of embryonic periods from stage 1 to 20. Confidence intervals represent the 95 percentile values from 1000 nonparametric bootstraps.

(86%) were included in the analysis (high: n = 339, low: n = 335).

Upon stocking the 2018 experiment, embryos ranged in stage from GS 1 to GS 10 (mean = GS 5.5), similar to the initial stages of embryos in the 2001 experiment (mean = 7.8, range = 3–11). Embryos were larger on average in 2018 (mean = 5.27 mL, SD = 1.0 mL) than in 2001 (mean = 4.2 mL, SD = 0.7 mL) (P < 0.001, Table S2). The models predicting embryonic period from repeated measures of developmental stage fit very well for both experimental years (Year [mR^2, cR^2]: 2001 [0.82, 0.98], 2018 [0.87, 0.98]) (Table 1, Fig. S7).

Our models of development estimate that an average embryo from the 2018 experiment attained hatching stage in 10.70 days in the low temperature treatment and 7.47 days in the high temperature treatment (Table S3). In comparison, the average embryonic period in the 2001 cohort was 12.46 days and 9.07 days, respectively (Table S3). Embryonic development was faster, and perforce, embryonic periods shorter in 2018 than 2001 by 1.7 days (−14.2%) for the low temperature treatment and 1.6 days (−17.6%) for the high temperature treatment (low: p < 0.001, high: p < 0.001; Table S3).

POND TEMPERATURE AND CANOPY

Our random forest model accounted for 87% of variance in daily pond temperatures with predictive accuracy within ±0.54°C of daily temperature. Across all ponds at our field site, pond water temperatures averaged an increase of 0.22 C (95% CI = 0.05–0.40) since 1999, in concordance with a 0.46°C rise in air temperature for the same seasonal window. However, temperature change during the embryonic period exhibited increases and decreases among populations, with extremes of similar magnitude (range = −0.33°C to 0.38°C) (Fig. 1C, Table S1). On average, canopies have become more closed, and consequently, ponds received 9.2% less light on average during the embryonic period in 2018 than in 2001 (range = −36.2 to 0.59) (Fig. 1C, Table S1). Although all ponds experienced positive or no change in canopy, there was no correlation between canopy change and temperature change during the embryonic period.

COUNTERGRADIENT VARIATION

The best fit model predicting embryonic period for the 2018 dataset included the interactive effects of pond temperature and canopy and fit much better than the next best model (ΔAIC = 39.6) (Table S4). The best fit model for the 2001 dataset included canopy but not temperature (Table S4); however, this model had only slightly better fit than the model with both environmental variables and the interaction (ΔAIC = 0.5). Thus, we report the results of the full model to be consistent with the 2018 results.

For experiments in both years, the effects of pond temperature and canopy were significant for embryos reared in the low-temperature treatment but not the high-temperature treatment (Table 2). This may be due to the increased range of embryonic periods resulting from protracted development in the low temperature treatment yielding higher power to discern

Table 2. Model results predicting embryonic period from spring pond temperatures (PondTemp), leaf-off canopy (Canopy), and treatment group ($Treatment_{Low}$, the High treatment is the baseline category) for the 2018 ($N_{observation}$ = 805, N_{pond} = 13) and 2001 ($N_{observation}$ = 674, N_{pond} = 11) experimental cohorts. Significant parameter estimates for which 95th percentile confidence intervals from 1000 nonparametric bootstraps do not contain zero are shown in bold.

	EP (2018)			EP (2001)		
Predictors	Estimates	CI	*P*	Estimates	CI	*P*
(Intercept)	6.64	–3.21 to 16.66	0.20	–2.13	–42.27 to 39.58	0.96
$Treatment_{Low}$	**–11.37**	**–15.62 to −7.21**	**<<0.01**	**–9.72**	**–20.75** to **−0.11**	**0.04**
PondTemp	0.04	–0.87 to 0.95	0.92	0.97	–3.00 to 4.57	0.62
Canopy	–0.02	–0.19 to 0.15	0.84	0.14	–0.43 to 0.69	0.64
$Treatment_{Low}$ * PondTemp	**1.46**	**1.08–1.86**	**<<0.01**	**1.09**	**0.18–2.12**	**0.01**
$Treatment_{Low}$ * Canopy	**0.22**	**0.15–0.29**	**<<0.01**	**0.19**	**0.06–0.33**	**<0.01**
PondTemp * Canopy	0.00	–0.01 to 0.02	0.79	–0.01	–0.06 to 0.04	0.66
$Treatment_{Low}$ * PondTemp * Canopy	**–0.02**	**–0.03 to −0.02**	**<<0.01**	**–0.02**	**–0.03 to 0.00**	**<0.01**
Random effects				**Random effects**		
σ^2	0.27			0.66		
$b_{0\ Pond}$	0.08			0.64		
Marginal R^2/ Conditional R^2	0.89/0.91			0.70/0.85		

Confidence intervals represent the 95 percentile values from 1000 nonparametric bootstraps.

differences. Here, we interpret the response among the low temperature treatment.

Among the 2018 cohort, holding canopy constant, we estimated embryonic periods increased by 0.32 day for ponds that are 1°C warmer, in a countergradient fashion (Fig. 2C). Functionally, this difference in intrinsic development rate predicts about a one day difference in embryonic period between the warmest and coldest ponds in our experiment. The effect of temperature is stronger in darker ponds. Among 2001 populations, we estimated embryonic periods to be longer by 0.19 day for 1°C warmer ponds (Fig. 2E).

Embryonic period, holding pond temperature constant, showed countergradient variation with respect to canopy in 2001 (Fig. 2F), but this relationship reversed in the 2018 experiment (Fig. 2D). For pond populations in 2018, we estimated embryonic periods to be 0.10 day shorter in ponds with 10% more canopy openness, but 0.30 day longer for the 2001 cohort (Table 2).

TEMPORAL COMPARISONS

Considering only the nine populations represented in both the 2001 and 2018 experiments, all populations exhibited faster development and reduced embryonic periods in both temperature treatments during the recent experiment (Fig. 3B). Compared to 2001, population-wise average embryonic periods evolved at a rate of −0.27 haldanes (range = −0.44 to −0.15) in the high temperature treatment and −0.15 haldanes (range = −0.38 to −0.03) in the low treatment, assuming a generation time of two years. All but one pond (BS) exhibited an increase in embryonic volume over time (Fig 3A) with an average increase of 1.05 mL (25%).

Our SEMs fit reasonably well, accounting for 54–57% of the variance in the difference in embryonic period across years (Table 3, Fig. 3C). For both temperature treatments, the greater the increase in pond temperature, the greater the increase in embryonic period across years. Thus, all ponds exhibited faster development over time, but those populations that experienced the least amount of warming relatively exhibited the most negative change in embryonic periods (i.e., greatest acceleration in developmental rates). Increases in embryonic volume elicited decreases in embryonic period, although this relationship was not significant for the high temperature treatment. There was no evidence that changes in canopy caused changes in pond temperature. Changes in canopy did not have a measurable effect on embryonic period directly nor mediated through the effect on embryonic volume.

LIMITS OF EVOLUTIONARY RESPONSE

There was a negative relationship between population growth and the pace of environmental change of natal ponds (Table 4, Fig. 4B). We estimate that, in general, populations that experience less than 0.87 standard deviations of change in temperature or canopy (or a combination thereof) exhibit stable or growing

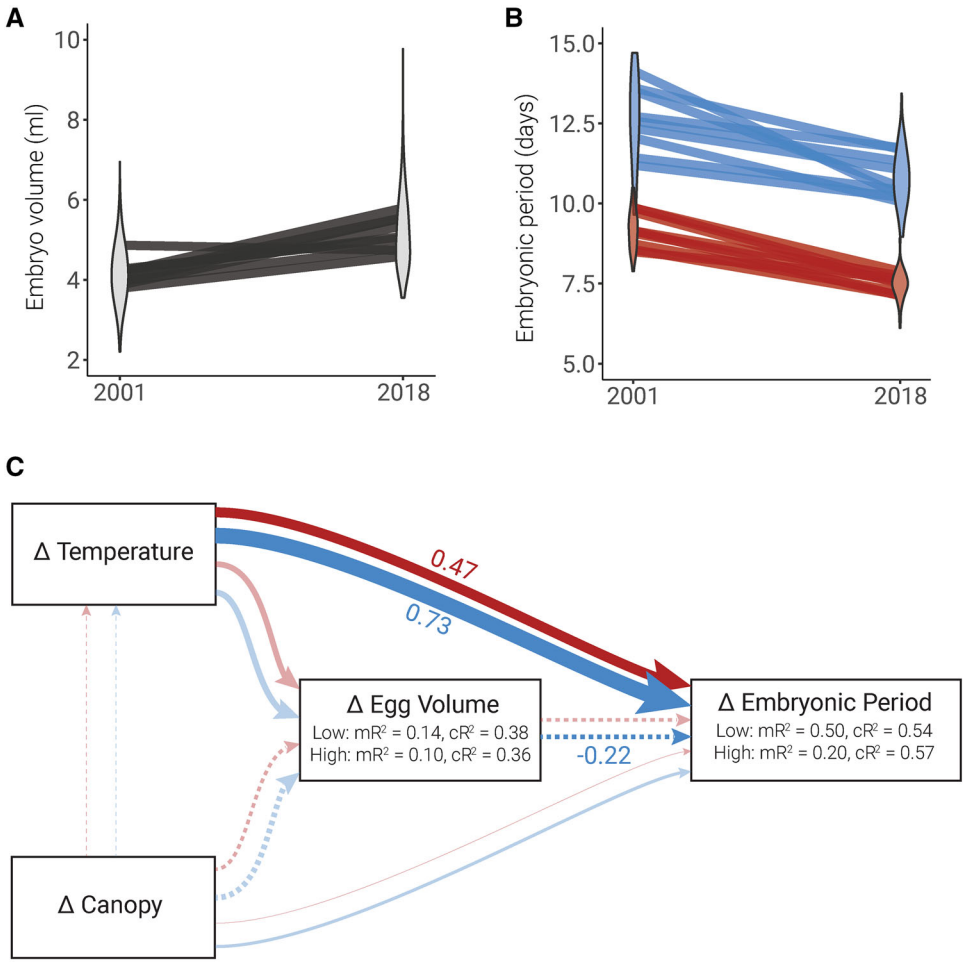

Figure 3. In general, embryonic volume increased (A) and embryonic periods decreased (B) between cohorts. Violin plots indicate overall change between cohorts, whereas lines between years show the change in means for each of the nine populations included in both the 2001 and 2018 common garden experiments. Structural equation models were used to estimate the strength and direction of variables hypothesized to cause a change in embryonic period (C). Paths in (C) represent directional causal paths. The widths of the paths are scaled to the standardized coefficient estimates. Solid paths indicate positive relationships, whereas dashed lines are negative. Significant paths are opaque and include standardized coefficient values, whereas nonsignificant paths are shown as transparent. Marginal and conditional coefficients of determination for piecewise models are shown. In all figures, colors represent high (red) and low (blue) temperature treatments.

Table 3. Results of structural equation model predicting the pond-wise change in embryonic period from 2001 to 2018. Significant piece-wise model parameters are indicated in bold.

		Low			High		
Response	Predictor	SE	Est.	*P* value	SE	Est.	*P* value
Δ Volume	Δ Canopy	–0.26	–0.04	0.09	–0.17	–0.03	0.27
Δ Volume	Δ Temp	0.28	1.44	0.07	0.27	1.4	0.08
Δ Temp	Δ Canopy	–0.04	0.00	0.92	–0.04	0.00	0.92
Δ EP	Δ Temp	**0.73**	**5.81**	**<<0.01**	**0.47**	**1.71**	**<0.01**
Δ EP	Δ Canopy	0.14	0.03	0.12	0.03	0.00	0.84
Δ EP	Δ Volume	**–0.22**	**–0.34**	**<0.01**	–0.17	–0.12	0.05
		Marginal R2/Conditional R2			Marginal R2/Conditional R2		
Δ Volume		0.14/0.38			0.10/0.36		
Δ Temp		0.00/NA			0.00/NA		
Δ EP		0.50/0.54			0.20/0.57		

Table 4. Model results estimating the relationship between environmental change (sum of absolute standardized change in pond temperature and canopy) and female breeding population size changes over time for wood frog populations at Yale Myers Forest ($N_{pond} = 14$, $N_{obs} = 266$). Significant parameter estimates for which 95th percentile confidence intervals from 1000 non-parametric bootstraps do not contain zero are shown in bold.

Predictors	Estimates	CI	*P*
Intercept	0.019	–0.003 to 0.050	0.5
Environmental change	**0.039**	**0.020–0.062**	**<0.01**
log(Year)	0.016	0.003–0.026	0.16
Environmental change * log(Year)	**–0.019**	**–0.028 to –0.011**	**<0.01**
Random effects			
σ^2	0.002		
$b_{0\ Pond}$	0.002		
$B_{1\ log(Year)}$	0.001		
$b_{0\ Pond:log(Year)}$	–0.001		
Marginal R^2/Conditional R^2	0.15/0.25		

Confidence intervals represent the 95 percentile values from 1000 nonparametric bootstraps.

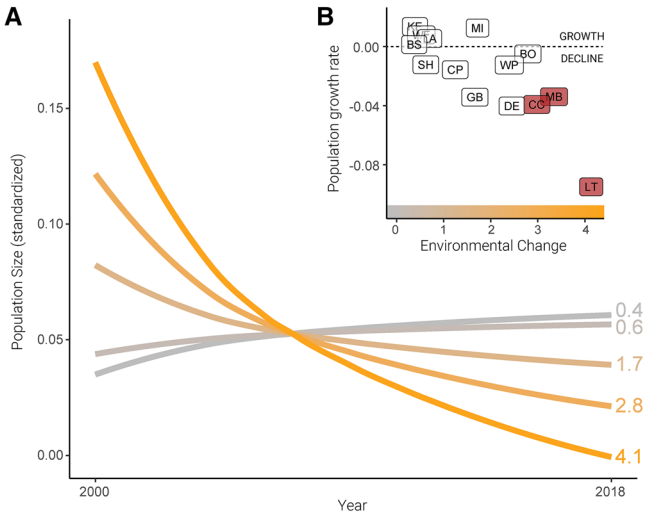

Figure 4. Population growth rates tend to decrease (B) and populations decline (A) with greater environmental change (sum of the scaled change in pond temperature and canopy). Growth curves (A) were predicted for the quartile values of environmental change experience by populations in the study. Conditional estimates of the log transformed slope of population growth (i.e., population growth rates) for each pond population are shown along the environmental change gradient in (B). Three pond populations that declined to extinction during the course of this study are indicated in red (B).

populations, while environmental change greater than that threshold leads to population declines (Fig. 4A). The three populations that went extinct prior to 2018 (MB, LT, and CC) experienced the greatest magnitude of environmental change (Fig. 1C) and some of the steepest population declines (Fig. 1D).

Discussion

A pattern of microgeographic variation first detected in 2001 persists in the same populations nearly two decades later. The results of our experiment affirm that evolution takes place over spatial scales easily traversed by an individual of our study species and that populations are evolving over time. Although Skelly (2004) was one of the first to document such microgeographic patterns, the phenomenon has since been observed in other systems (Richardson et al. 2014) and, owing to the cryptic nature of countergradient variation, is likely to be uncovered in still more as further field research is carried out. Within the context of climate change, our fundamental finding that a species is capable of rapid, fine-scale evolution in response to thermal variation should provide a reason to expect that adaptation to changing climate is possible and may insulate species from some of its consequences. Although that is a reasonable interpretation, we also have evidence to conclude that there are limits to such adaptation and that the failure of evolutionary rescue may be linked to the extinction of some populations (Fig. 4; Klausmeier et al. 2020).

Despite the complexity of environmental change taking place between 2001 and 2018 (canopy closure, increased water temperature, period of intense drought), the relationship between embryonic period and temperature in our experiment conformed to expectations based on the pattern of countergradient variation seen in 2001. Most critically, embryos from warmer ponds took relatively longer to develop, whereas embryos from colder ponds developed relatively more rapidly. However, in absolute terms, embryonic periods decreased overall from 2001 to 2018, whereas temperatures across the site increased. This result violates both expectations from space-for-time inference and expectations that selection would erode spatial gradients over time as selection drives populations at the maladapted end of the gradient to extinction.

One potential explanation for this counterintuitive difference between spatial and temporal gradients is that while accelerated development may be advantageous in general, there may be trade-offs when organisms develop too quickly (Gahm et al. 2021). The microgeographic pattern uncovered in 2001 showed that populations in the warmest ponds exhibited depressed intrinsic development rates relative to those in colder ponds. Given warming and canopy change over time, selection may have favored faster development across the metapopulation as a whole, leading to shorter embryonic periods overall. However, those

population that faced large increases in temperature more quickly may have approached the threshold at which accelerated development results in performance costs, limiting their ability to adapt and attenuating the resultant shift in embryonic development across timepoints.

The potential for populations to circumvent extinction through evolutionary rescue has become even more salient in the face of anthropogenic climate change. Despite the general focus on climate, our results suggest that landscape change can interact with climate change in important ways. Since 2001, ponds tended to become darker as the surrounding canopy matured. The effect of shading did not have a straightforward effect on spring pond temperature, perhaps because other factors influence water temperature, such as ground water and snowmelt runoff. In fact, the direction of the relationship between canopy closure and embryonic development reversed between experimental years. Although embryos developed more quickly in darker ponds in 2001, embryos from more open ponds tended to develop most quickly in 2018. Notably, our SEMs did not indicate that changes in canopy resulted in changes in embryonic period directly nor mediated through change in egg volume. Three ponds populations that failed prior to 2018 exhibited some of the largest shifts in canopy, but consequently were not included in the SEM dataset. The compound effects of canopy closure and increasing air temperatures may impact wood frog development indirectly, however, by altering the hydroperiod of breeding ponds.

Both higher air temperature and denser canopies lead to increased evaporation and evapotranspiration of vernal pools (Brooks and Hayashi 2002), especially after deciduous leaves emerge. The shift to warmer air and pond water temperature and darker canopies is much greater for the larval period than the spring embryonic period (Arietta et al. 2020 and Supporting Information figures). The net result is likely a decrease in hydroperiod.

The aquatic developmental period of wood frogs is limited to the ice-free hydroperiod of vernal pools. Oviposition occurs shortly after the surface ice melts and larvae must metamorphose prior to the pond drying out. Although climate warming allows some species to maintain the developmental window by commencing breeding earlier in the spring, this is not possible at our site during at least some years because more persistent snowpack counterintuitively delays oviposition (Arietta et al. 2020). Thus, constricting hydroperiods would exert extreme selective pressure for faster development to avoid mass mortality events when ponds desiccate prior to metamorphosis. There is considerable experimental evidence of plastic and genetic effects on developmental timing in response to hydroperiod (Richter-Boix et al. 2011; Lent and Babbitt 2020).

In addition to shifts in embryonic period, embryonic volume has also shifted over time. Across amphibians as a group, larger embryos are associated with faster development (Bradford 1990). We see this same relationship—within a given cohort, larger embryos tend to develop more quickly (i.e., shorter embryonic periods), and between cohorts, the increase in embryo size is associated with a decrease in embryonic periods.

The shift to larger embryos partially counteracts the direct effect of increases in temperature on embryonic periods in our populations. Interestingly, the SEMs did not indicate that changes in embryo size were a result of shifts in pond temperature nor canopy. Nevertheless, climate may have played a role in shifting embryonic size. The interim period between our experiments saw some of the most extreme drought conditions in the past century. Droughts may have selected for larger, older females who are better able to cope with water balance due to smaller surface area-to-volume ratio and lower area-specific evaporative water loss rate (Claussen 1969). In ranid frogs, there is a strong, positive correspondence between the size and age of females and larger embryos (Berven 1988).

Although we see evidence that populations exhibit putatively adaptive shifts in intrinsic embryonic development rate, it is notable that three populations that did not persist between experimental years (MB, CC, and LT) also experienced the greatest changes in canopy and temperature (Fig. 4). For both the embryonic and larval period, "LT" saw the greatest increase in canopy closure, but moderate change in temperature. "MB" and "CC" saw the greatest increase and decrease in temperature, respectively, but moderate canopy closure. "DE," a pond with comparable change to "CC," has seen declining populations since 2001. Yet, these ponds are not outliers in temperature or canopy. It will be worth exploring further whether it is the pace of changes in conditions, and not the conditions per se, that determine population persistence and the extent to which microevolutionary adaptation can rescue populations. Current methods of predicting species range shifts in the future focus almost entirely on changes in habitat suitability but not the pace at which it occurs (Wiens et al. 2009). Thus, this is a critical question for conservation management and reveals the importance of tracking evolutionary responses over time.

Despite the power of allochronic common garden studies to demonstrate responses to contemporary climate change (Hendry and Kinnison, 1999), very few researchers have undertaken such experiments to date (Merilä and Hendry 2014). One reason is the difficulty of exactly replicating experimental conditions between timepoints. Despite using the same incubators in both experimental years, the daily variation in rearing temperatures was lower in 2018 than in 2001 and the mean temperature was slightly higher. Embryonic development in ectotherms is influenced by both mean temperature and fluctuation in temperature in nonadditive ways (Massey and Hutchings 2021). We corrected for the shift in mean temperature analytically, but could not

correct for variance. At moderate temperatures like those used in our experiment, both theory (Liu and Meng 2000; Georges et al. 2005; Massey and Hutchings 2021) and empirical findings (e.g., Niehaus et al. 2006; Arrighi et al. 2013; Hall and Warner 2020) suggest that temperature fluctuations have either no effect or cause accelerated development rates. In our experiments, we find the opposite, embryos in 2001 experience more thermal variability yet slower development that embryos in 2018, making it unlikely that the differences we see are a result of experimental conditions.

A second reason replication is rarely attempted is the inherent difficulty in defining any field ecology study conducted over time as truly "direct" replication, given that all ecology takes place on a nonreplicated planet (Filazzola and Cahill 2021). In our case, this same problem means that it is impossible to conclusively state that allochronic difference are the result of evolution and not artifacts. However, our study approached direct replication as closely as possible and multiple lines of evidence point to interesting biological change.

The extent to which the pace and scale of microevolution will play a role in conservation and management of biodiversity in the future is an open question (Stockwell et al. 2003). Answering it will require ongoing theory and empirical studies of evolutionary responses to climate change. Vernal pond species are particularly vulnerable to climate change because their developmental window is time-constrained by development rates, which are closely tied to water temperatures. Unlike other organisms, vernal pool species cannot simply migrate upstream or down the water column to cooler waters and are relatively isolated over very small spatial scales. Thus, adaptation is the only recourse, making vernal pool species excellent models to understand the limits of adaptation to climate change. This study joins a growing body of research showing that contemporary evolution is common and often rapid relative to ecological processes. Although there are limits on the extent to which evolution and plasticity can buffer climate change (Radchuk et al. 2019), this study suggests a potential role for evolutionary rescue in circumventing biodiversity loss in some cases.

AUTHOR CONTRIBUTIONS

AA conducted the experiments and analysis. AA and DS conceived of the study and wrote the manuscript.

ACKNOWLEDGMENTS

We would like to thank Adriana Rubinstein, Dr. L. Kealoha Freidenburg, and Greg Watkins-Colwell for their generous help with lab and field work. Thanks to Dr. Freya Rowland, Dr. Nate Edleman, Yara Alshwairikh, Dahn-Young Dong, Logan Billet, and Dr. Annise Dobson for early reviews of this manuscript. Funding for this study was provided by Yale Institute for Biospheric Studies and Yale Forests Kohlberg-Donohoe Research Fellowship. Animal handling and collections were approved by Yale University IACUC (2004-10361, 2016-10361, 2019-10361, 2006-11024, 2009-11024, 2009-11040) and Connecticut DEEP (205001, 211001b, 0112019d). Field work was conducted with permission from Yale Myers Research Committee (SKE01, AND17).

DATA ARCHIVING

The data that support the findings of this study are openly available in Dryad at https://doi.org/10.5061/dryad.08kprr53b.

CONFLICT OF INTEREST

The authors declare no conflict of interest.

LITERATURE CITED

Anderson, M. C. 1964. Studies of the woodland light climate I. The photographic computation of light condition. J. Ecol. 52:27–41.

Arietta, A. Z. A. & D. K. Skelly 2021. Data from: Rapid microgeographic evolution in response to climate change. Evolution. https://doi.org/10.5061/dryad.08kprr53b

Arietta, A. Z. A., L. K. Freidenburg, M. C. Urban, S. B. Rodrigues, A. Rubinstein, and D. K. Skelly. 2020. Phenological delay despite warming in wood frog *Rana sylvatica* reproductive timing: a 20-year study. Ecography 52:27. https://doi.org/10.1111/ecog.05297

Arrighi, J. M., E. S. Lencer, A. Jukar, D. Park, P. C. Phillips, and R. H. Kaplan. 2013. Daily temperature fluctuations unpredictably influence developmental rate and morphology at a critical early larval stage in a frog. BMC Ecol. 13:18.

Barton, K. 2019. MuMIn: multi-model inference. https://CRAN.R-project.org/package=MuMIn

Bates, D., M. Mächler, B. Bolker, and S. Walker. 2015. Fitting linear mixed-effects models using lme4. J. Statist. Softw. 67:1–48.

Berven, K. A. 1988. Factors affecting variation in reproductive traits within a population of wood frogs (*Rana sylvatica*). Copeia 1988:605–615.

———. 2009. Density dependence in the terrestrial stage of wood frogs: evidence from a 21-year population study. Copeia 2009:328–338.

Berven, K. A., D. E. Gill, and S. J. Smith-Gill. 1979. Countergradient selection in the green frog, *Rana clamitans*. Evolution 33:609–623.

Bolnick, D. I., and P. Nosil. 2007. Natural selection in populations subject to a migration load. Evolution 61:2229–2243.

Bradford, D. F. 1990. Incubation time and rate of embryonic development in amphibians: the influence of ovum size, temperature, and reproductive mode. Physiol. Zool. 63:1157–1180.

Bradshaw, W. E., and C. M. Holzapfel. 2001. Genetic shift in photoperiodic response correlated with global warming. PNAS 98:14509–14511.

Brooks, R. T., and M. Hayashi. 2002. Depth-area-volume and hydroperiod relationships of ephemeral (vernal) forest pools in southern New England. Wetlands 22:247—255.

Carlson, S. M., C. J. Cunningham, and P. A. H. Westley. 2014. Evolutionary rescue in a changing world. Trends Ecol. Evol. 29:521–530.

Catullo, R. A., J. Llewelyn, B. L. Phillips, and C. C. Moritz. 2019. The potential for rapid evolution under anthropogenic climate change. Curr. Biol. 29:R996–R1007.

Claussen, D. L. 1969. Studies on water loss and rehydration in anurans. Physiol. Zool. 42:1–14.

Conover, D. O., and E. T. Schultz. 1995. Phenotypic similarity and the evolutionary significance of countergradient variation. Trends Ecol. Evol. 10:248–252.

Ficetola, G. F., and F. Bernardi. 2005. Supplementation or in situ conservation? Evidence of local adaptation in the Italian agile frog Rana latastei

and consequences for the management of populations. Anim. Conserv. 8:33–40.

Filazzola, A., and J. F. Cahill Jr. 2021. Replication in field biology: identifying challenges and proposing solutions. Methods Ecol. Evol. https://doi.org/10.1111/2041-210X.13657

Frazer, G. W., C. D. Canham, and K. P. Lertzman. 1999. Gap Light Analyzer (GLA): Imaging software to extract canopy structure and gap light transmission indices from true-color fisheye photographs, users manual and documentation (Version 2.0). Simon Fraser University. http://rem-main.rem.sfu.ca/downloads/Forestry/GLAV2UsersManual.pdf

Gahm, K., A. Z. A. Arietta, and D. K. Skelly. 2021. Temperature-mediated trade-off between development and performance in larval wood frogs (*Rana sylvatica*). J. Exp. Zool. A 335:146–157.

Gaitán-Espitia, J. D., and A. J. Hobday. 2020. Evolutionary principles and genetic considerations for guiding conservation interventions under climate change. Global Change Biol. https://doi.org/10.1111/gcb.15359

Georges, A., K. Beggs, J. E. Young, and J. S. Doody. 2005. Modelling development of reptile embryos under fluctuating temperature regimes. Physiol. Biochem. Zool. 78:18–30.

Gienapp, P., C. Teplitsky, J. S. Alho, J. A. Mills, and J. Merilä. 2008. Climate change and evolution: disentangling environmental and genetic responses. Mol. Ecol. 17:167–178.

Gomulkiewicz, R., and R. D. Holt. 1995. When does evolution by natural selection prevent extinction? Evolution 49:201–207.

Gosner, K. L. 1960. A simplified table for staging Anuran embryos and larvae with notes on identification. Herpetologica 16:183–190.

Hall, J. M., and D. A. Warner. 2020. Ecologically relevant thermal fluctuations enhance offspring fitness: biological and methodological implications for studies of thermal developmental plasticity. J. Exp. Biol. 223(Pt 19). https://doi.org/10.1242/jeb.231902

Hendry, A. P., and M. T. Kinnison. 1999. Perspective: the pace of modern fife: measuring rates of contemporary microevolution. Evolution 53:1637–1653.

Hoffmann, A. A., and C. M. Sgrò. 2011. Climate change and evolutionary adaptation. Nature 470:479–485.

Kawecki, T. J., and D. Ebert. 2004. Conceptual issues in local adaptation. Ecol. Lett. 7:1225–1241.

Kinnison, M. T., and A. P. Hendry. 2001. The pace of modern life II: from rates of contemporary microevolution to pattern and process. Genetica 112–113:145–164.

Klausmeier, C. A., M. M. Osmond, C. T. Kremer, and E. Litchman. 2020. Ecological limits to evolutionary rescue. Philos. Trans. R. Soc. Lond. B Biol. Sci. 375:20190453.

Lefcheck, J. S. 2016. piecewiseSEM: Piecewise structural equation modelling in R for ecology, evolution, and systematics. Methods Ecol. Evol./Br. Ecol. Soc. 7:573–579.

Lent, E., and K. J. Babbitt. 2020. The effects of hydroperiod and predator density on growth, development, and morphology of wood frogs (*Rana sylvatica*). Aquat. Ecol. 54:369–386.

Liaw, A., and M. Wiener. 2002. Classification and regression by randomForest. R News 2:18–22. https://CRAN.R-project.org/doc/Rnews/

Liu, S. S., and X. D. Meng. 2000. Modelling development time of *Lipaphis erysimi* (Hemiptera: Aphididae) at constant and variable temperatures. Bull. Entomol. Res. 90:337–347.

Massey, M. D., and J. A. Hutchings. 2021. Thermal variability during ectotherm egg incubation: a synthesis and framework. J. Exp. Zool. A Ecol. Integr. Physiol. 335:59–71.

Meester, L. D., R. Stoks, and K. I. Brans. 2018. Genetic adaptation as a biological buffer against climate change: potential and limitations. Integr. Zool. 13:372–391.

Merilä, J., and A. P. Hendry. 2014. Climate change, adaptation, and phenotypic plasticity: the problem and the evidence. Evol. Appl. 7:1–14.

Muir, A. P., R. Biek, R. Thomas, and B. K. Mable. 2014. Local adaptation with high gene flow: temperature parameters drive adaptation to altitude in the common frog (*Rana temporaria*). Mol. Ecol. 23:561–574.

Nevo, E., Y.-B. Fu, T. Pavlicek, S. Khalifa, M. Tavasi, and A. Beiles. 2012. Evolution of wild cereals during 28 years of global warming in Israel. PNAS 109:3412–3415.

Niehaus, A. C., R. S. Wilson, and C. E. Franklin. 2006. Short- and long-term consequences of thermal variation in the larval environment of anurans. J. Anim. Ecol. 75:686–692.

Orizaola, G., M. Quintela, and A. Laurila. 2010. Climatic adaptation in an isolated and genetically impoverished amphibian population. Ecography 33:730–737.

Radchuk, V., T. Reed, C. Teplitsky, M. van de Pol, A. Charmantier, C. Hassall, P. Adamík, F. Adriaensen, M. P. Ahola, P. Arcese et al. 2019. Adaptive responses of animals to climate change are most likely insufficient. Nat. Commun. 10:3109.

Razgour, O., B. Forester, J. B. Taggart, M. Bekaert, J. Juste, C. Ibáñez, S. J. Puechmaille, R. Novella-Fernandez, A. Alberdi, and S. Manel. 2019. Considering adaptive genetic variation in climate change vulnerability assessment reduces species range loss projections. PNAS 116:10418–10423.

Reznick, D. N., J. Losos, and J. Travis. 2019. From low to high gear: there has been a paradigm shift in our understanding of evolution. Ecol. Lett. 22:233–244.

Richardson, J. L., M. C. Urban, D. I. Bolnick, and D. K. Skelly. 2014. Microgeographic adaptation and the spatial scale of evolution. Trends Ecol. Evol. 29:165–176.

Richter-Boix, A., M. Tejedo, and E. L. Rezende. 2011. Evolution and plasticity of anuran larval development in response to desiccation. A comparative analysis. Ecol. Evol. 1:15–25.

Rowland, F., Schyling, E., Richardson, J., Arietta, A. Z. A., Rodrigues, S., Rubinstein, A., Freidenburg, L. K., Urban, M. C., Skelly, D. K., and M. Benard. (in review). Asynchrony, density dependence, and persistence in amphibian populations. Ecology.

Sala, O. E., F. S. Chapin 3rd, J. J. Armesto, E. Berlow, J. Bloomfield, R. Dirzo, E. Huber-Sanwald, L. F. Huenneke, R. B. Jackson, A. Kinzig et al. 2000. Global biodiversity scenarios for the year 2100. Science 287:1770–1774.

Schiffers, K., E. C. Bourne, S. Lavergne, W. Thuiller, and J. M. J. Travis. 2013. Limited evolutionary rescue of locally adapted populations facing climate change. Philos. Trans. R. Soc. Lond. B Biol. Sci. 3681610. 20120083.

Schneider, C. A., W. S. Rasband, and K. W. Eliceiri. 2012. NIH image to ImageJ: 25 years of image analysis. Nat. Methods 9:671–675.

Skelly, D. K. 2004. Microgeographic countergradient variation in the wood frog, *Rana sylvatica*. Evolution 58:160–165.

Stockwell, C. A., A. P. Hendry, and M. T. Kinnison. 2003. Contemporary evolution meets conservation biology. Trends Ecol. Evol. 18: 94–101.

Thornton, P. E., M. M. Thornton, B. W. Mayer, Y. Wei, R. Devarakonda, R. S. Vose, and R. B. Cook. 2016. Daymet: daily surface weather data on a 1-km grid for North America, Version 3. ORNL Distributed Active Archive Center. https://doi.org/10.3334/ORNLDAAC/1328

Urban, M. C. 2015. Climate change. Accelerating extinction risk from climate change. Science 348:571–573.

Werner, E. E., D. K. Skelly, R. A. Relyea, and K. L. Yurewicz. 2007. Amphibian species richness across environmental gradients. Oikos 116:1697–1712.

Wiens, J. A., D. Stralberg, D. Jongsomjit, C. A. Howell, and M. A. Snyder. 2009. Niches, models, and climate change: assessing the assumptions and uncertainties. PNAS 106(Suppl 2), 19729–19736.

Associate Editor: A. Siepielski
Handling Editor: A. G. McAdam

Supporting Information

Additional supporting information may be found online in the Supporting Information section at the end of the article.

Figure S1. Comparison of spring (A, leaf-off) and spring + summer (B, weighted mean leaf-on and leaf-off over wood frog aquatic development period) canopy closure estimates (GSF = Global Site Factor) for 14 wood frog breeding ponds averaged over 2–172 photos captured at the intersection of 5 m cartesian grids (Cartesian Grid) or a subsample of five photos captured at the four cardinal points and center (Cardinal Points) of each pond during 1999 and 2000 seasons. Colors indicate ponds that are represented in both experimental timepoints (black), only the 2001 experiment (red), and only the 2018 experiment (gray).

Figure S2. The number of daily observations across all 34 ponds and 18 years (2001–2019) included in the random forest training dataset.

Figure S3. Decrease in error, estimated by out-of-bag cross-validation, for increasing numbers of trees included in the random forest model predicting daily pond water temperature.

Figure S4. Importance of variable in predictive accuracy of the random forest model prediction daily pond water temperatures measured by the percentage decrease in mean square error of the out-of-bag cross-validation estimates when each variable is included (A) and the total decrease in node impurity (i.e., number of correctly estimated leaves) by splitting on each variable (B).

Table S1. Change in environmental variables between the 2001 and 2018 experiments.

Figure S5. Change in pond temperature in relation to canopy for 14 wood frogs ponds between 2001 and 2018 for spring (A) and spring and summer (B) seasonal windows.

Figure S6. Change in pond temperature in relation to canopy for 16 wood frogs ponds between 2001 (point) and 2018 (label) for spring (A) and spring and summer (B) seasonal windows.

Figure S7. Embryonic development rates of wood frog embryos collected within 24 h of oviposition in 2001 (A) and 2018 (B) and reared in incubators representing high (red) or low (blue) temperatures experienced across natal ponds until hatching (approximately Gosner state 20).

Figure S8. Embryonic period duration for each embryo was estimated from developmental growth rates corrected for differences in realized incubator temperatures.

Table S2. Mixed effect model results testing for difference in initial embryo volume between 2001 and 2018 experiment with random intercepts for clutchmates nested within pond.

Table S3. Mixed effect model results testing for difference in initial embryonic period between 2001 and 2018 experiment with random intercepts for ponds.

Table S4. Model selection table predicting embryonic period by leaf-off canopy (Can) and spring water temperatures (Temp) for the 2001 and 2018 experimental cohorts and vary with temperature treatment (Treat).

Figure S9. Partial effect plots for embryonic period duration estimated with linear mixed effect models for 2018 (top row, A and B) and 2001 (bottom row, C and D) cohorts when reared in a common garden at high (red) and low (blue) temperature treatments.

Table S5. Mixed effect regression results for estimating the effect of larval period pond temperatures (PondTemp) and spring and summer canopy cover (Canopy) on embryonic period for the 2018 and 2001 experimental cohorts.

Table S6. Exposition of causal assumption tested by the structural equation models.